Open Archive TOULOUSE Archive Ouverte (OATAO)

OATAO is an open access repository that collects the work of Toulouse researchers and makes it freely available over the web where possible.

Molecular mobility in piezoelectric hybrid nanocomposites with 0–3 connectivity: Volume fraction influence

Jean-Fabien Capsal [a], Eric Dantras [b,*], Jany Dandurand [b], Colette Lacabanne [b]

[a] *Piezotech S.A.S., 9 rue de Colmar, 68220 Hésingue, France*
[b] *Physique des Polymères, Institut CARNOT-CIRIMAT, Université Paul Sabatier, 31062 Toulouse, France*

ABSTRACT

Thermo Stimulated Current and Dynamic Dielectric Spectroscopy studies were carried out on hybrid ferroelectric Polyamide 11/Barium Titanate to investigate dielectric relaxation modes. The correlated results obtained by both methods allow us to describe precisely the molecular mobility of this 0–3 nanocomposite; in this work we will focus on the influence of the 700 nm nanoparticles volume fraction. The dielectric spectroscopy shows that the molecular mobility associated with the liquid dynamic is not influenced by the volume fraction. The evolution of low frequency relaxation, observed by depolarization currents techniques, have been attributed to the decrease of Cooperative Rearranging Region size and the increase of intra/inter macromolecular interactions in the soft amorphous phase.

1. Introduction

Since the discovery of the ferroelectric behavior of some class of polymers [1–6], these materials have attracted great interest for their good piezo/pyroelectric properties, low permittivity, lightweight and ductility. These materials have potential applications in sensor and electromechanical transduction. However, the poling field required to give a ferroelectric property to these materials is high [7–9]. This high poling field could restrict their use in some particular cases. Ferroelectric ceramics such as Barium titanate are commonly known for their high electroactive properties and low poling field [10,11]. To overcome the disadvantage of high poling field of organic ferroelectrics, inorganic particles are dispersed in a polymeric matrix to obtain a 0–3 connectivity composite in Newnham notation [12]. Previous works have shown that the piezo/pyroelectric properties of these composites have a poling field more than 20 times lower than ferroelectric polymers [13–17]. The final electroactive properties of these composites are close to organic materials and conserve the ductility of the matrix [18].

As far as we know, very few works have been devoted to the influence of the inorganic phase on the physical structure of the organic amorphous phase. In this study we report the volume fraction influence of inorganic ferroelectric barium titanate (700 nm) on the molecular dynamics of the amorphous phase of a polyamide 11. Broadband Dielectric Spectroscopy and Thermo Stimulated Current have been used to check the physical structure of these composites at a nanometric scale in a wide frequency range.

2. Experimental

2.1. Samples elaboration

The mean diameter of Barium titanate ($BaTiO_3$) nanoparticles is 700 nm. Polyamide 11 (PA 11) powder was dissolved in a solution of dimethyl acethyl amide (DMAc) and the required barium titanate powder was dispersed to form a mixture by ultrasonic stirring. The samples were dried over night at 110 °C to remove the solvent. The nanocomposites were hot pressed to form thin films of 70 to 100 μm thick. Volume fractions (ϕ) of nanoceramic in nanocomposite films were ranging from 0.03 to 0.45.

The dispersion of barium titanate nanopowder in the polymeric matrix has been studied by Scanning Electron Microscopy (SEM) in order to check the experimental protocol. Fig. 1 shows cryo-cut images of PA11/$BaTiO_3$ 700 nm nanocomposites for 12%, 24%, 45% and 58% in volume. A homogeneous dispersion at nanometric scale is observed until a volume fraction of 45%. For $\phi = 58\%$, nanoparticles aggregation is observed; that could be responsible of a decrease of mechanical properties.

2.2. Dielectric experiments

Thermostimulated Currents (TSC) thermograms were carried out on a TSC/RMA Analyser. For complex thermograms, the sample was polarized by an electrostatic field during $t_p = 2$ min over a temperature range from the polarization temperature $T_p = 90$ °C down to the freezing

* Corresponding author.
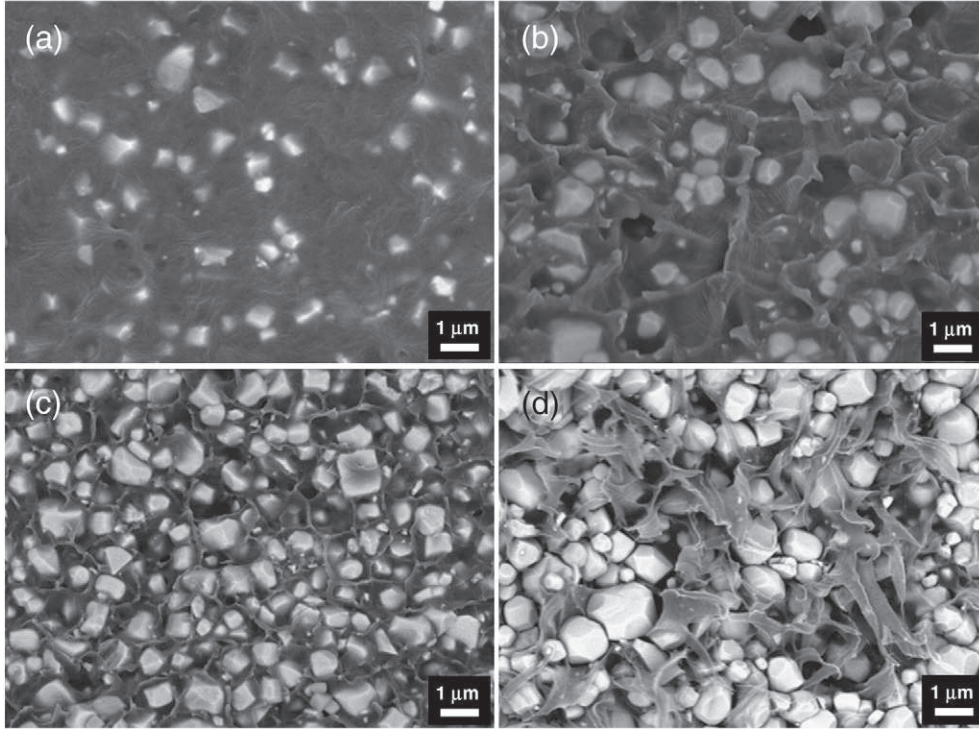*E-mail address:* dantras@cict.fr (E. Dantras).

Fig. 1. Scanning Electron Microscope (SEM) images of PA11/BaTiO$_3$ 700 nm composites with $\phi = 12\%$ (a), 24% (b), 45% (c), 58% (d).

temperature T$_0$. Then the field was turned off and the depolarization current was recorded with a constant heating rate (q$_h$ = +7 °C·min^{-1}), the equivalent frequency of the TSC spectrum was f$_{eq}$ ~ 10^{-2}–10^{-3} Hz. Elementary TSC thermograms were performed with a poling window of 5 °C. Then the field was removed and the sample cooled at a temperature T$_{cc}$ = T$_p$ − 30 °C. The depolarization current was recorded with a constant heating rate (q$_h$ = +7 °C·min^{-1}). Each elementary thermogram was recorded by shifting the poling window 5 °C toward higher temperature.

Dynamic dielectric spectroscopy (DDS) were performed using a BDS400 covering a frequency range of 10^{-2} Hz − 3.10^6 Hz with 10 points per decade. Experiments were carried out in a temperature range from − 150 °C to 150 °C. Dielectric isothermal spectra were measured every 2 °C. Before each frequency scan, temperature was kept constant to ± 0.2 °C. The real ε′$_T$ and imaginary ε″$_T$ parts of the relative complex permittivity ε*$_T$ were measured as a function of frequency f at a given temperature T. The complex dielectric permittivity ε* was fitted by the Havriliak–Negami function:

$$\varepsilon^*(\omega) = \varepsilon_\infty + \frac{(\varepsilon_s - \varepsilon_\infty)}{(1 + (i\omega\tau)^{\beta_{HN}})^{\gamma_{HN}}}$$

Where ε$_s$ is the static permittivity, ε$_\infty$ is the permittivity at high frequency, and β$_{HN}$, γ$_{HN}$ are the Havriliak–Negami parameters.

3. Results

In this section, the volume fraction influence of 700 nm BaTiO$_3$ nanoparticles is observed by DDS and TSC on the molecular mobility of the PA 11 amorphous part. The volume fraction ϕ of BaTiO$_3$ in PA 11 is ranging from 0% to 58%.

3.1. Dielectric relaxation modes in dynamic spectroscopy

The isothermal relaxations modes have been characterized by DDS. Prior to measurements and to prevent any plasticization phenomena causes by water absorption of aliphatic polyamides [18] the composites were dehydrated along 4 h at 110 °C. Volume fraction influence on the conservative (ε′) and dissipative part (ε″) of the dielectric permittivity have been studied.

Fig. 2a shows the frequency dependence of ε′ for the isotherm T = 26 °C. The volume fraction is ranging from 0% to 45%. The conservative part of the polyamide 11 dielectric permittivity is ε′ = 2.5 at f = 1 kHz and slightly decrease with the frequency. Barium titanate is known for its high dielectric permittivity [19] (ε′ ~ 1500 at 25 °C). As the inorganic BaTiO$_3$ nanoparticles are dispersed into the organic matrix, the dielectric permittivity of the composite highly increases with ϕ. Dielectric permittivity is increasing from 3 for 3% to 10 for 45% in volume. In the same way the frequency evolution of the permittivity between 0.1 Hz and 1 MHz (Δε = ε′ (1 MHz) − ε′ (0.1 Hz)) is enhanced by the volume fraction of inorganic phase; i.e. Δε = 0.75 for polyamide 11 and is multiplied by 2 for 24% in volume.

As the conservative part of the permittivity, the dielectric loss ε″ is modified by the inorganic volume fraction. Fig. 2b shows the frequency dependence of ε″ at T = 26 °C. The dielectric loss of the polyamide matrix at 1 MHz is ε″ = 0.035. As the volume fraction of barium titanate increases from 3% to 24%, the dielectric losses increase from 0.042 to 0.07. For 45%, ε″ slightly decrease but is still higher than the dielectric loss of the matrix.

Fig. 3 reports the thermal dependence of the dielectric permittivity of PA11/BaTiO$_3$ (58% in volume) for various frequencies ranging from 74 kHz to 1 MHz. Two dielectric phenomena are pointed out. The first one is attributed to the dielectric manifestation of the polyamide glass transition (α mode). The second one at 130 °C cannot be distinguished until a volume fraction up to 45%. This relaxation is not thermally activated and so can be associated with the inorganic phase. The temperature position and frequency dependence of this phenomenon are consistent with the dielectric manifestation of the nanoparticles Curie transition [19,20]. Below 45% in volume, the dielectric behavior of PA11/BaTiO$_3$ 700 nm composites is governed by the organic phase predominantly. Above ϕ = 45% a competition between inorganic and organic component appears; a complex dielectric spectra is composed of both phases responses results.

The analytical fit of the dielectric permittivity ε* (ε* = ε′ − iε″) with Havriliak–Negami equation [21] allows us to extract the

(a)

(b)

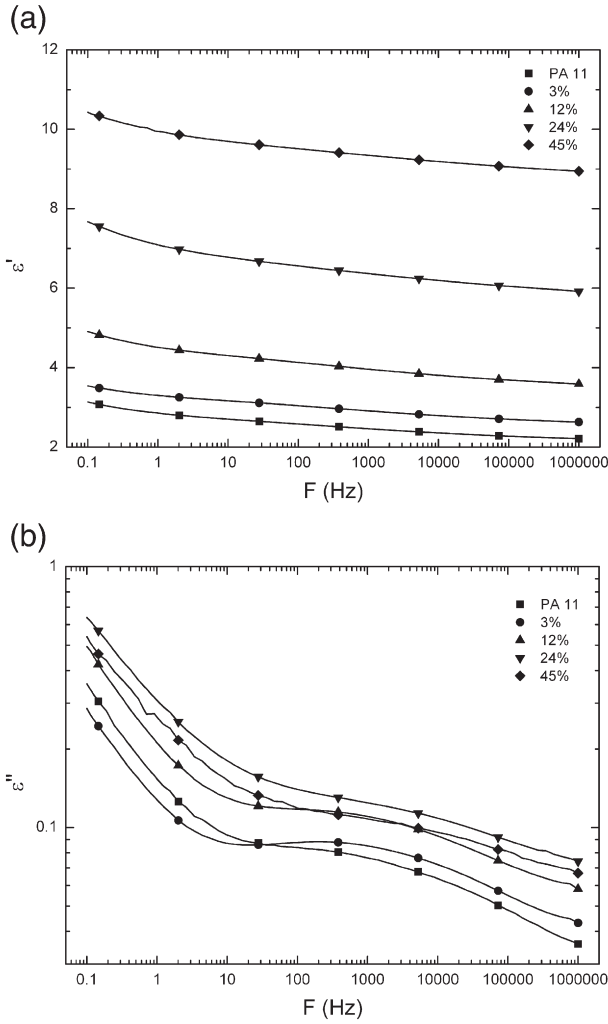**Fig. 2.** Frequency dependence of ε′ (a) and ε″ (b) measured at T = 26 °C for φ = 0%, 12%, 24% and 45%.

relaxations times τ_{HN} associated with the polyamide 11 dipolar relaxations. As previously report [20], in this temperature and frequency range PA 11 is characterized by 4 modes called γ, β, α and α′. In this study we focus on the dielectric relaxations γ, α and α′. The β mode, generally associated with the water amide complex has not be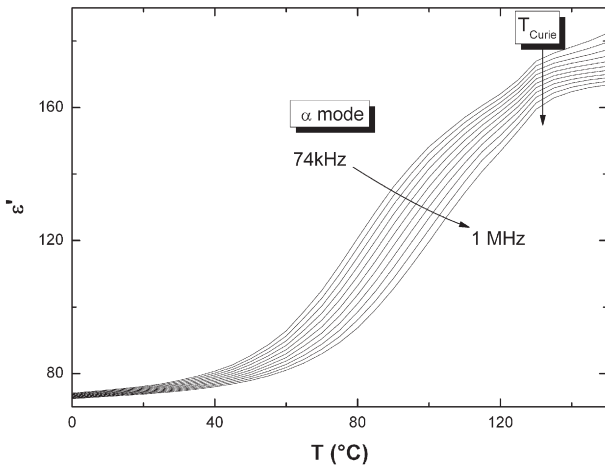en studied due to inherent evolution of this relaxation mode with water. Heterogeneous systems such as semi-crystalline polymers are generally characterized at low frequency and high temperature by an important increase of the dielectric permittivity. This process is known as Maxwell–Wagner– Sillars (MWS) phenomenon [22]. The increase of ε″ due to MWS process could hinder dipolar relaxation involved at high temperature. In order to avoid this issue, the dielectric modulus formalism has been used to extract the relaxations times of high temperature dielectric relaxation (α′ and MWS).

Fig. 4 shows a high temperature isotherm T = 80 °C of dielectric loss for permittivity (ε″) and modulus (M″) for PA11/BaTiO$_3$ 700 nm composite with φ = 24%. For dielectric permittivity two relaxations modes are pointed out (α and α′) with an important increase of ε″ in the low frequency range (MWS process and/or conductivity phenomenon). With dielectric modulus formalism, three dielectric phenomena are identified. This formalism allows a better resolution of α′. The MWS process is characterized by a peak which gives an opportunity to follow the influence of particles volume fraction on this process.

The Arrhenius diagram of the composites is reported in Fig. 5 as function of φ. The relaxation times of the γ, α, α′ modes and MWS are reported. γ and α relaxations have been fitted in the permittivity formalism; α′ and MWS in the modulus formalism.

The γ mode has an Arrhenius behavior while α is characterized by a Vogel–Tammann–Fulcher (VTF) temperature dependence. The pre-exponential factor τ_0, the activation energy E_a and the VTF parameters are reported in Table 1. The activation energy of sub vitreous γ relaxation of PA 11 is $E_a = 49$ kJ·mol^{-1} with a pre-exponential factor $\tau_0 = 1.10^{-7}$ s. The activation energy slightly decreases with the introduction of the barium titanate particles: from 46 kJ·mol^{-1} for φ = 12% to 38 kJ·mol^{-1} for φ = 45%. The evolution with φ of τ_0 is opposite. τ_0 increases from 4.10^{-17} s to 8.10^{-16} s respectively. VTF parameters of the α mode are not dependant from the volume fraction. The dielectric relaxation associated with the dielectric manifestation of the glass transition is not influenced by the volume fraction.

The α′ mode follows a VTF behavior. This relaxation process is attributed to the molecular mobility of constrained amorphous phase near the PA 11 crystalline regions. The dispersion of BaTiO$_3$ into the polyamide has a weak influence on the molecular dynamic of this mode. Nevertheless the α′ relaxation times are slightly shifted toward higher times with φ increases; it has been associated with a weak decrease of this constrained amorphous phase molecular mobility.

The MWS contribution is strongly influenced by the introduction of the BaTiO$_3$ particles. As the particles volume fraction increases, the relaxation times of this relaxation process are shifted toward longer times indicating that free carriers require more thermal energy to be trapped in the amorphous/crystalline boundaries of the organic phase.

Fig. 3. Real part of the dielectric permittivity versus temperature of PA 11/BaTiO$_3$ 700 nm nanocomposites with φ = 58%.

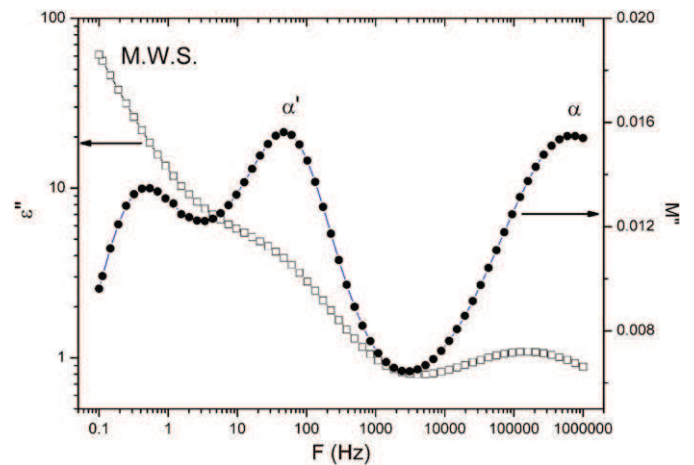**Fig. 4.** Frequency dependence of the dissipative part of the dielectric permittivity ε″ (□) and dielectric modulus M″ (●) measured at T = 80 °C for φ = 24%.
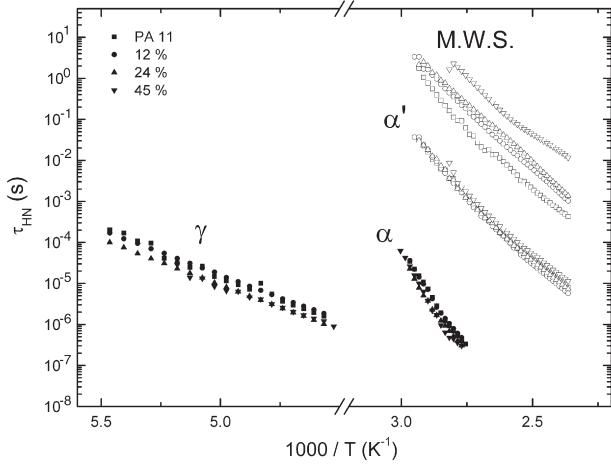
Fig. 5. Relaxation map of PA 11/BaTiO₃ 700 nm composites extract from Havriliak–Negami equation using the dielectric permittivity formalism for γ and α relaxations (full symbols) and the dielectric modulus formalism for α′ relaxation and MWS (open symbols).

3.2. Dielectric relaxation modes in thermal analysis

The evolution of the non isothermal relaxation processes have been characterized by TSC. Prior to the measurements, the samples were heated up to 140 °C for 30 min to prevent any plasticization effect due to water absorption of the polyamide. As we only focus on the influence of the BaTiO₃ particles on the molecular mobility of the organic matrix, TSC thermograms were normalized to the volume fraction of organic phase.

Fig. 6 shows the TSC thermograms of PA11/BaTiO₃ 700 nm in a temperature range from -150 °C to 0 °C with ϕ ranging from 3% to 24%. The samples have been polarized under an electric field of $3\,MV\cdot m^{-1}$ ($t_p = 2$ min) at 0 °C and then short-circuited at -160 °C. In this temperature range, only one relaxation β_1 has been pointed out for polyamide 11 at $T_\beta = -50$ °C. This process is attributed to the dipolar relaxation of the free amide groups in the amorphous phase. A shoulder in low temperature tail $T_{\beta 2} = -80$ °C of the TSC thermogram is observed. This mode is associated with the mobility of "water-amide" complexes. BaTiO₃ particles do not influence the temperature position of the relaxation processes. However, the β relaxations amplitude ($\sigma_{\beta max}$) decreases; i.e. $\sigma_{\beta max}$ of PA11/BaTiO₃ with $\phi = 24\%$ is diminished by 50% compare to polyamide.

Complex TSC thermogram of the β modes with $\phi = 12\%$ and the elementary processes associated with this relaxation are shown in Fig. 7a. Elementary processes follow the global thermal evolution of the complex thermogram. Two maxima attributed to β_1 and β_2 dipolar relaxations are pointed out. From the fractional TSC thermograms the characteristic activation parameters of these processes are extracted.

The activation enthalpies ΔH (with an uncertainty of 5%) as function of temperature for PA11/BaTiO₃ composites are reported on

Table 1
Arrhenius parameters of γ relaxation and VTF parameters of α relaxation of PA11/BaTiO₃ composites with $\phi = 0\%$, 12%, 24%, 45%.

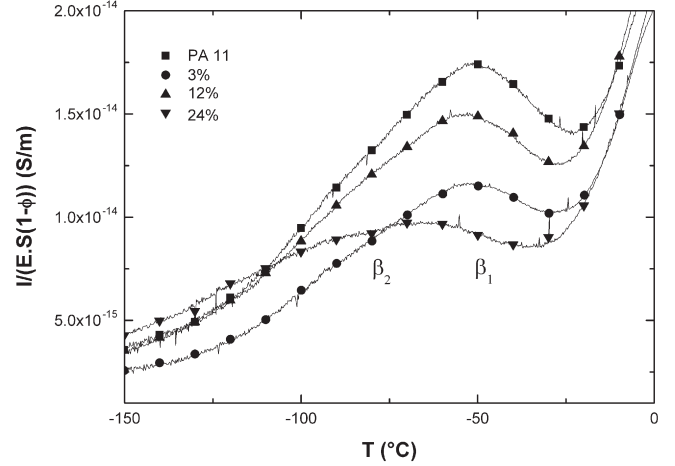| Volume fraction ϕ	γ model τ_0 (s)	γ mode E_a (kJ/mol)	α mode τ_0 (s)	α mode α (K⁻¹)	α mode T_0 (K)	α mode $D = 1/\alpha T_0$
PA 11	$1 \cdot 10^{-17}$	49 ± 1	$8 \cdot 10^{-11}$	$2 \cdot 10^{-3}$	293 ± 15	1.9
12%	$4 \cdot 10^{-17}$	46 ± 0.5	$6 \cdot 10^{-12}$	$1 \cdot 10^{-3}$	275 ± 10	3.5
24%	$8 \cdot 10^{-17}$	42 ± 1	$1 \cdot 10^{-10}$	$2 \cdot 10^{-3}$	292 ± 3	1.9
45%	$8 \cdot 10^{-16}$	38 ± 0.5	$7 \cdot 10^{-10}$	$3 \cdot 10^{-3}$	308 ± 7	1.03

Fig. 6. Low temperature TSC thermograms normalized to the volume fraction of organic phase for PA 11 and $\phi = 3\%$, 12% and 24% ($T_p = 0$ °C, $T_0 = -160$ °C).

Fig. 8. The null activation entropy dependence of the enthalpies [23] (called Starkweather "line") is also reported. β modes are characterized by a linear dependence of ΔH. Whatever the volume fraction of inorganic phase in the composite the enthalpies of these processes
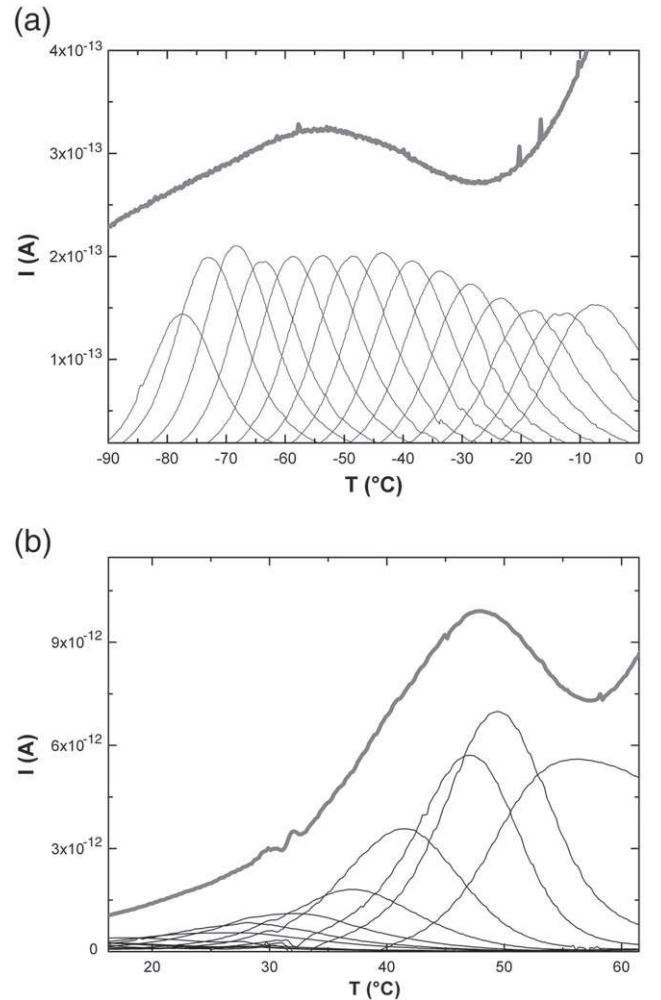

Fig. 7. TSC thermogram (gray line) and elementary thermograms (black line) of (a) β mode for $\phi = 12\%$ and (b) α mode for $\phi = 24\%$.
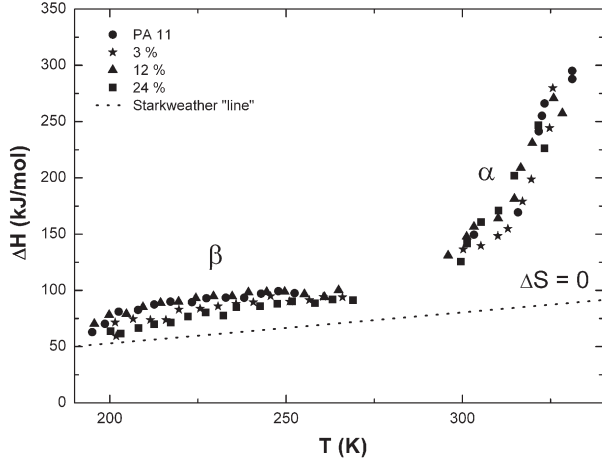
Fig. 8. Enthalpy versus temperature extract from elementary TSC thermograms for $\phi = 0\%$, 3%, 12% and 24% (symbols) and Starkweather "line" (dashed line).

follow the Starkweather "line". It means that the molecular mobility of β relaxations remains localized and not influenced by BaTiO₃.

For high temperature TSC experiments, the composites were polarized under an electric field $E_p = 0.5 \, MV \cdot m^{-1}$ at $T_p = 80 \, °C$ and short-circuited at $T_{cc} = 0 \, °C$. Fig. 9 shows the high temperature thermograms of PA11/BaTiO₃ composites with ϕ ranging from 0% to 45%. Only one relaxation mode (α mode) is pointed out whatever the volume fraction. This primary relaxation is occurring at $T_\alpha = 55 \, °C$ for PA11. As T_α is in the same temperature range than the calorimetric glass transition, the α relaxation is attributed to the dielectric manifestation of PA11 glass transition. T_α and σ_{max} linearly decreases with ϕ. For $\phi = 24\%$, the decrease of T_α is 10 °C and σ_{max} is reduced by 50% compare to pure PA 11.

Fig. 7b reports the fractional and complex TSC thermograms of composites with $\phi = 24\%$. The shape of elementary thermograms is coherent with the complex thermogram. From the fractional experiments, activation enthalpies ΔH of each elementary relaxation is determined and reported on Fig. 8 for ϕ ranging from 0% to 24%. For α relaxation activation enthalpies diverged from the null activation entropy line. It is consistent with delocalized cooperative mobility. However, the maximum enthalpy ΔH decreases with ϕ which indicates that the molecular mobility is more localized as ϕ increases.

4. Discussion

4.1. Slow relaxation processes

The relaxations times obtained by DDS and associated with the MWS phenomena are influenced by the dispersion of inorganic particles. As ϕ increases, τ_{HN} (MWS) are shifted toward longer relaxation times. MWS is attributed to free charges carriers trapping at the boundaries of heterogeneities below the glass transition temperature. This process is highly dependent from the conductivity of the composite above Tg. BaTiO₃ is an electrically insulate material. When the volume fraction increases, the high temperature conductivity of the composite decreases and so it requires more thermal energy for free carriers to be trapped near the heterogeneities. Due to time-temperature equivalence, more thermal energy means longer relaxation times. So the evolution of MWS with ϕ is attributed to the influence of the particles on the electric conductivity of the composites.

4.2. PA 11/BaTiO₃ 700 nm composites connectivity

Fig. 10 shows the real part of the dielectric permittivity ε' versus the volume fraction of BaTiO₃ particles (room temperature, f = 1 kHz). The experimental values have been fitted with the Bruggeman model [24]. For $\phi < 45\%$, the experimental data are well fitted. According to this model, one can extract the dielectric permittivity of the inorganic part of the composite. From Bruggeman model, ε' of BaTiO₃ 700 nm is evaluated to be nearly 1500. This value is in good agreement with bulk ceramic sintered from BaTiO₃ 700 nm nanoparticles using Spark Plasma Sintering technique. For $\phi > 50\%$, the experimental points departs from the Bruggeman model. For these high volume fractions the connectivity [12] of the biphasic system is modified by the agglomeration of nanoparticles. 0–3 connectivity, in Newnham notation, does not govern the physical properties of the composite. For $\phi > 50\%$, 3–3 connectivity described the dispersion of inorganic nanoparticles in the polyamide matrix. This point is in good agreement with the observation of the Curie dielectric manifestation of the inorganic phase for $\phi > 50\%$, and with Scanning Electron Microscopy analysis.

4.3. Structural evolution of the organic amorphous phase

The decrease of the α mode amplitude obtained by TSC with the increase of inorganic phase has been attributed to the immobilization of a polyamide amorphous phase fraction. This point is in good agreement with Differential Scanning Calorimetry measurements performed on these composites [17]. ΔCp associated with Tg decreases with the

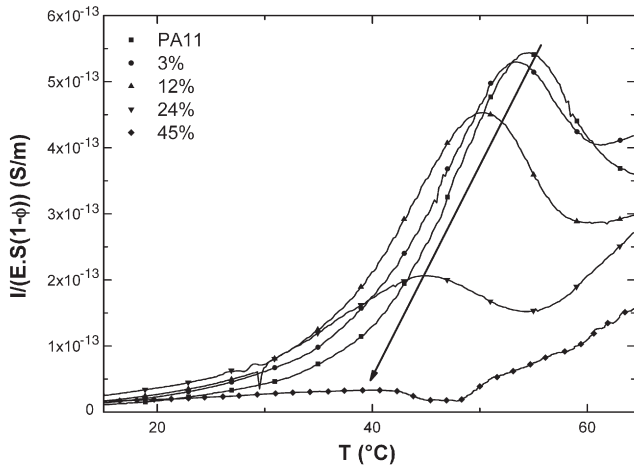**Fig. 9.** High temperature TSC thermograms normalized to the volume fraction of organic phase for PA 11 and $\phi = 3\%$, 12% and 24% ($T_p = 80 \, °C$, $T_0 = 0 \, °C$).
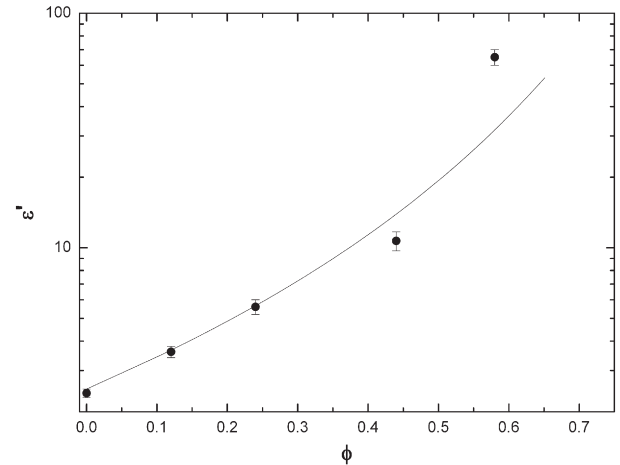

Fig. 10. Conservative part of the dielectric permittivity ε' versus volume fraction ϕ and analytical fit with the Bruggeman model (solid line).
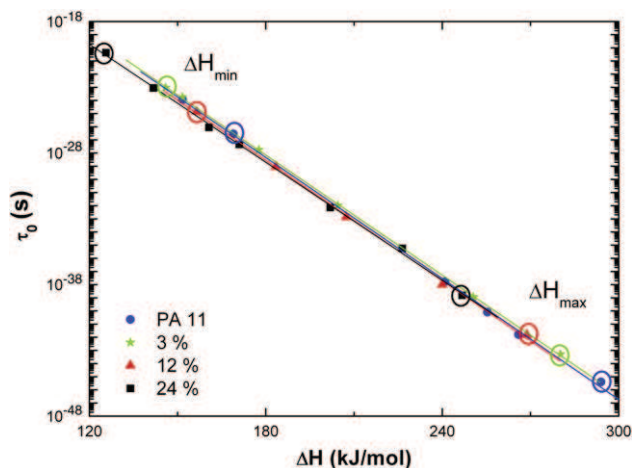
Fig. 11. Pre-exponential factor (τ_0) versus enthalpy extract from elementary TSC thermograms of α mode for PA11/BaTiO$_3$ 700 nm composites with $\phi = 0\%$, 3%, 12% and 24%.

increase of ϕ. Due to the low interactions between inorganic and organic phase of the composites, the immobilization of polyamide amorphous phase has been attributed to the increase of intra and inter macromolecular interactions induced by high densification of the matrix with ϕ.

The main influence of the nanoparticles on the polyamide matrix reports in this study concerned the variation of dipolar relaxation enthalpies of the amorphous phase, extracted from elementary TSC thermograms, near the vitreous transition. An important decrease of the maximal and minimal enthalpies of the α relaxation mode with ϕ is shown on composites.

Fig. 11 illustrates the evolution of the pre-exponential factor τ_0 (proportional to activation entropy ΔS) versus activation enthalpy extracted from fractional TSC thermograms of α mode as function of ϕ. For each volume fraction a compensation phenomenon is pointed out. The compensation times τ_c and compensation temperature T_c deduced for PA 11 are $\tau_c = 2 \cdot 10^{-2}$ s and $T_c = 75$ °C ($T_g + 20$ °C). The volume fraction does not influence the compensation parameters of α mode. Open circles on Fig. 11 mark the maximum and minimum values of activation enthalpy. PA 11 has a maximal enthalpy $\Delta H_{max} = 293$ kJ·mol^{-1} and a minimal one $\Delta H_{min} = 151$ kJ·mol^{-1}. As ϕ increases, the maximum and minimum ΔH values decrease; i.e. ΔH_{max} decreases from 279 kJ·mol^{-1} for $\phi = 3\%$ to 246 kJ·mol^{-1} for $\phi = 24\%$. In a same way, ΔH_{min} is decreased by 30% for a volume fraction of 24%. The decrease of activation enthalpies values with ϕ is attributed to the reduction of Cooperative Rearranging Regions (CRR) size [25] due to the high densification of the matrix with the inorganic phase content. However, the BaTiO$_3$ 700 nm particles are assumed to have an infinite size compare to CRR (few nanometers [26]).

5. Conclusion

The present study describes the influence of inorganic nanofillers on the physical properties of the polymeric matrix of PA11/BaTiO$_3$ 0–3 nanocomposites. The volume fraction of BaTiO$_3$ particles increases the conservative and dissipative part of the dielectric permittivity. The evolution of ε' with ϕ is well described by Bruggeman model until $\phi = 45\%$. Above this inorganic content, a divergence between experimental data and Bruggeman model is observed mainly caused by a change in connectivity from 0–3 to 3–3. The molecular mobility in the liquid state is not perturbed by BaTiO$_3$ fillers. In the glassy state, a slight evolution of the soft organic amorphous phase has been pointed out. The important densification of the composite with ϕ induces a decrease of the CRR size observed thanks to enthalpy values. The amplitude of the TSC α mode decreases with ϕ which is consistent with an immobilization of a part of the amorphous phase of the polyamide matrix caused by an increase of intra/inter macromolecular interactions.

Acknowledgements

References

[1] H. Kawai, Japanese Journal of Applied Physics 8 (1969) 975.
[2] A.J. Lovinger, Science 220 (1983) 1115.
[3] M. Oshiki, E. Fukada, Journal of Materials Science 10 (1975) 1.
[4] L. Ibos, A. Bernes, C. Lacabanne, Ferroelectrics 320 (2005) 48.
[5] R.J. Klein, J. Runt, Q.M. Zhang, Macromolecules 36 (2003) 7220.
[6] H.M. Bao, J.F. Song, J. Zhang, Q.D. Shen, C.Z. Yang, Q.M. Zhang, Macromolecules 40 (2007) 2371.
[7] G.A. Samara, F. Bauer, Ferroelectrics 135 (1992) 385.
[8] J.I. Scheinbeim, J.W. Lee, B.A. Newman, Macromolecules 25 (1992) 3529.
[9] J.F. Capsal, E. Dantras, J. Dandurand, C. Lacabanne, Polymer 51 (2010) 4606.
[10] T.A. Perls, T.J. Diesel, D.W. Dobrov, Journal of Applied Physics 29 (1958) 1297.
[11] W.R. Cook, D.A. Berlincourt, F.J. Scholz, Journal of Applied Physics 34 (1963) 1392.
[12] R.E. Newnham, D.P. Skinner, L.E. Cross, Material Research Bulletin 13 (1978) 525.
[13] K.A. Hanner, A. Safari, R.E. Newnham, Runt, J Ferroelectrics 100 (1989) 255.
[14] T. Furukawa, K. Fujino, E. Fukada, Japonese Journal of Applied Physics 15 (1976) 2119.
[15] C.J. Dias, D.K. Das Gupta, IEEE Transactions on Dielectrics and Electrical Insulation 3 (1996) 706.
[16] J.F. Capsal, E. Dantras, L. Laffont, J. Dandurand, C. Lacabanne, Journal of Non-Crystalline Solids 356 (2010) 629.
[17] J.F. Capsal, C. Pousserot, E. Dantras, J. Dandurand, C. Lacabanne, Polymer 51 (2010) 5207.
[18] H.W. Starkweather Jr., G.E. Moore, J.E. Hansen, T.M. Roder, R.E. Brooks, Journal of Polymer Science 21 (1956) 189.
[19] S.G. Fritsch, M. Boulos, B. Durand, V. Bley, T. Lebey, Journal of the European Ceramic Society 25 (2005) 2749.
[20] J.F. Capsal, E. Dantras, J. Dandurand, C. Lacabanne, Journal of Non-Crystalline Solids 353 (2007) 4437.
[21] S. Havriliak, S. Negami, Polymer 8 (1967) 161.
[22] F. Kremer, A. Schönals, Broad Band Dielectric Spectroscopy, Springer, Berlin, 2003.
[23] H.W. Starkweather, Macromolecules 14 (1981) 1277.
[24] D.A.G. Bruggeman, Annalen der Physik 24 (1935) 636.
[25] E. Donth, Journal of Non-Cristalline solids 307 (2002) 364.
[26] A. Saiter, N. Delpouve, E. Dargent, J.M. Saiter, European Polymer Journal 43 (2007) 4675.